RSC Advances

Cite this: *RSC Advances*, 2012, **2**, 7617–7632

www.rsc.org/advances

REVIEW

Hierarchical structure and mechanical properties of nacre: a review

Jiyu Sun[ab] and Bharat Bhushan*[a]

Received 7th February 2012, Accepted 3rd May 2012
DOI: 10.1039/c2ra20218b

Nacre (known as mother of pearl) is the iridescent inner shell layer of some mollusks. Nacre is composed of 95 wt% aragonite (a crystallographic form of $CaCO_3$) and 5 wt% organic materials (proteins and polysaccharides). It is well known that it exhibits high fracture toughness, much greater than that of monolithic aragonite, because of its ingenious structure. It also exhibits energy absorption properties. It has a complex hierarchical microarchitecture that spans multiple length scales from the nanoscale to the macroscale. It includes columnar architectures and sheet tiles, mineral bridges, polygonal nanograins, nanoasperities, plastic microbuckling, crack deflection, and interlocking bricks, which exhibit a remarkable combination of stiffness, low weight and strength. Nacre's special self-assembly characteristics have attracted interest from materials scientists for the development of laminated composite materials, molecular scale self-assembly and biomineralization. This paper reviews the characteristics of hierarchical structure and the mechanical properties of nacre that provide the desired properties, and the latest developments and biomimetic applications.

1 Introduction

The hard shells of mollusks have adapted to their living conditions to protect their soft bodies against external aggression from predators, rocks or debris displaced by currents or waves.[1] The shell anatomies of two classes of mollusk, bivalves and gastropods, are shown in Fig. 1 and 2. It generally consists of a three-layered structure:[2–4] the outermost layer is periostracum (composed of hardened protein), the middle layer is prismatic (composed of columnar calcite), and the inner layer is nacre (also known as mother of pearl, composed of aragonite, which is a crystallographic form of $CaCO_3$ and organic materials). The exterior layers of the shell are typically brittle and hard, which can provide resistance to penetration from external impact, while nacre provides toughening by dissipating the mechanical energy, owing to its capability for undergoing large inelastic deformations.[5–8]

Of the nacre-producing mollusks, bivalves and gastropods are the most common and have been studied the most.[1,9] Some species of mollusk do not have nacre, such as *Meretrix lusoria* (bivalves) and *Pecten maximus* (bivalves).[10] Table 1 shows some mollusk shells that consist of nacre.

Nacre is composed of 95 wt% aragonite (a crystallographic form of $CaCO_3$) and 5 wt% organic materials (proteins and polysaccharides). Although the organic matrix in nacre is only 5 wt%, it plays an important role in spatial and chemical control of the crystal nucleation and growth, microstructure and toughness enhancement.[11,12] For example, fracture toughness of nacre is 3.3–9 MPa $\sqrt{m}$, which is about three to nine times that of monolithic aragonite (about 1 MPa $\sqrt{m}$).[13–17] Nacre has been investigated for several decades due to its exceptional mechanical properties, ability to self-assemble and complex hierarchical structure, which spans the nanometer to millimeter length scales.[6,8,9,12,18–30]

Nacre consists of a brick-and-mortar like structure, in which hard aragonite tablets are glued together with soft organic materials to form tiles.[25,31,32] Lamellar micro-architectures of hard composite tiles with soft organic layers in between can be thought of as 'ceramic plywood', which causes crack deflection and resists slip in order to provide toughness and impact resistance. The architecture of nacre spans from molecular, mineral bridges,[33–37] to nanoscale, polygonal nanograins,[38,39] nanoasperities,[40] and interlocked bricks,[41] over the atomic to the tens of microns length scale, with strengthening and toughening mechanisms associated with each length scale. In the literature, many studies on nacre can be found that have been conducted to investigate the reasons behind its enhanced properties.[22,42]

It should be pointed out that different shell-forming mollusks consist of different inner structures with varying mechanical properties.[43] In general, investigations of the mechanical properties of biological materials can be divided into two major groups: (1) microscale and nanoscale indentation (mechanical properties such as elastic modulus, hardness, and toughness are determined *via* indentation methods); and (2) miniaturized bulk mechanical testing (compression, bending or tensile experiments for elastic modulus, strength and toughness).[44] Most research in nacre consists of investigation of its micro-mechanical properties.[5,13,25,44–48] Recently, with an interest in nanotechnology, the mechanical properties of nacre on the nanoscale have been investigated.[17,49–53] Nanoindentation on even individual tablets has been performed.[49,54]

[a]*Key Laboratory of Bionic Engineering (Ministry of Education), Jilin University, Changchun, 130025, P. R. China*
[b]*Nanoprobe Laboratory for Bio- & Nanotechnology and Biomimetics (NLB2), The Ohio State University, 201 W. 19th Avenue, Columbus, OH 43210-1142, USA. E-mail: Bhushan.2@osu.edu, sjy@jlu.edu.cn*

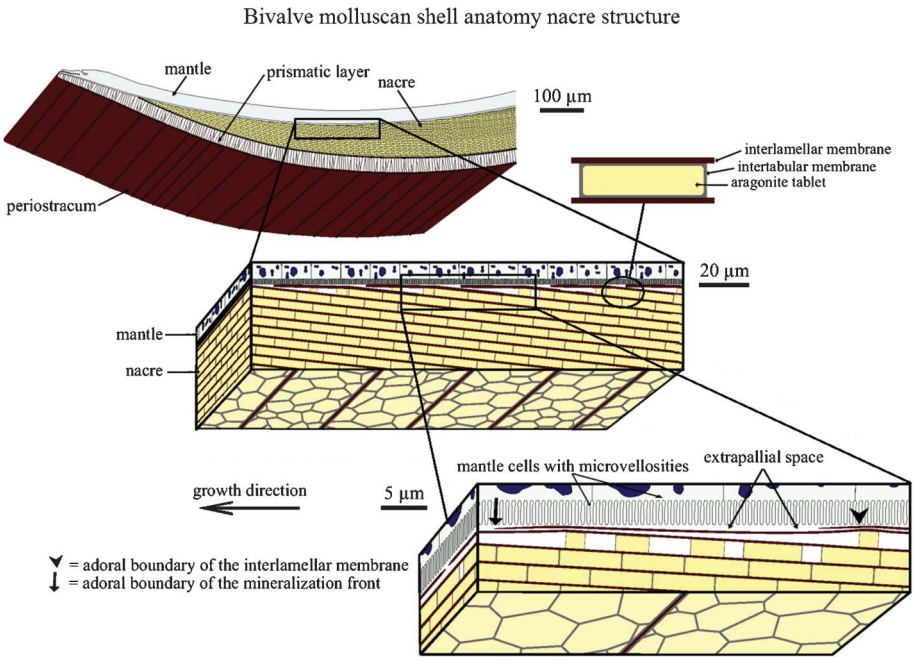

Fig. 1 Schematic of the bivalve molluscan shell anatomy. It is composed of periostracum, a prismatic layer and nacre. The liquid-filled interlamellar space exists between the mineralized shell and the mantle part of the soft body of the organism. The schematic also illustrates successive amplifications of the brick and mortar structure of nacre. The growth surface, on which the patterns are observed, is between the mantle and the shell, and extends into the page.[3]

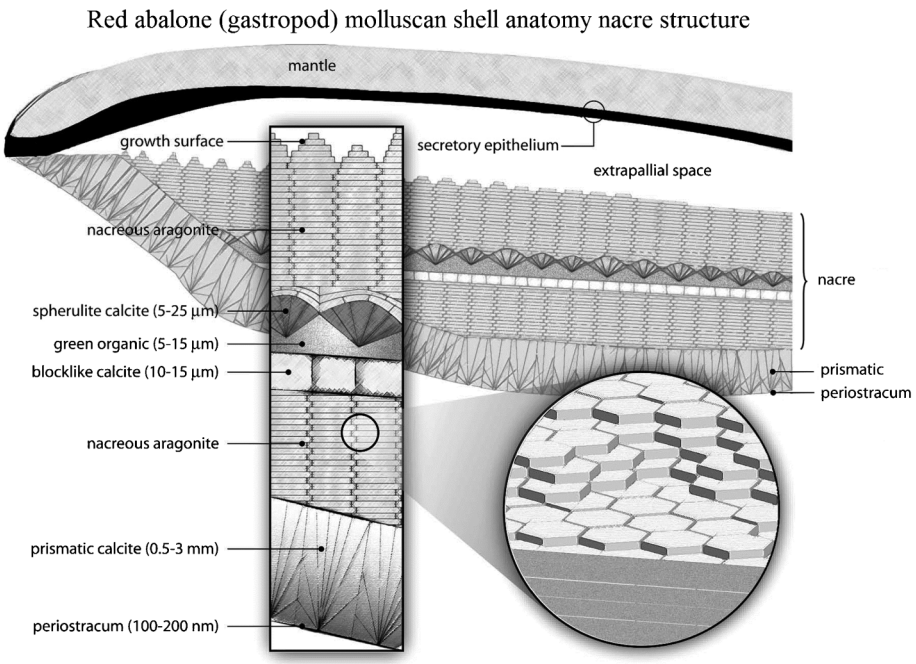

Fig. 2 Schematic of the red abalone (gastropod) molluscan shell anatomy, showing a vertical section of the outer edge of the shell and mantle with an enlargement indicating the thickness dimensions of the shell structures. The size of the extrapallial space is exaggerated for clarity.[2,112]

As an excellent source of inspiration, nacre has opened a way to inspire new ideas for fabricating novel materials and structures, such as biomimetic coatings,[55] free standing films[18,56–61] and composite materials.[1,59,62–73]

In this paper, we present a review of the characteristics of the hierarchical structure and mechanical properties of nacre which provide the desired properties, and the latest developments and biomimetic applications.

Table 1 Classification of some mollusk shells that consist of nacre

Class	Family	Genus	Species	References
Bivalves	Meretricinae	*Meretrix*	*Meretrix lusoria*	Fleischli *et al.*[10]
	Mytilidae	*Bathymodiolus*	*Bathymodiolus azoricus*	Machado *et al.*[114]
		Perna	*Perna canaliculus* (green mussel)	Leung and Sinha;[106] Pokroy *et al.*;[115] Moshe-Drezner *et al.*[110]
		Modiolus	*Modiolus modiolus*	Currey[45]
	Nuculidae	*Nucula*	*Nucula nitidosa*	Cartwright and Checa;[9] Checa *et al.*[37,94]
	Pinnidae (pen shell)	*Atrina*	*Atrina pectinata*	Cartwright and Checa[9]
			Atrina rigida	Nudelman *et al.*[88]
			Atrina vexillum	Currey[45]
	Pteriidae	*Pteria*	*Pteria avicula*	Cartwright and Checa;[9] Cartwright *et al.*[3] Fig. 1
			Pteria hirundo	Cartwright and Checa;[9] Cartwright *et al.*[3]
			Pteria penguin	Fleischli *et al.*[10]
		Pinctada (pearl oysters)	*Pinctada maxima*	Stempflé and Brendlé;[107] Stempflé *et al.*;[116] Wang *et al.*[5]
			Pinctada margaritifera	Chateigner *et al.*;[83] Checa *et al.*;[94] Currey;[45] Currey *et al.*;[117] Jackson *et al.*;[13] Rousseau *et al.*[101]
			Pinctada sp.	Currey[45]
	Tellinidae	*Tellinella*	*Tellinella asperrima*	Ren *et al.*[118]
	Unionidae	*Anodonta*	*Anodonta cygnea* (swan mussel)	Cartwright and Checa;[9] Currey;[45] Machado *et al.*[114]
		Hyriopsis	*Hyriopsis schlegeli*	Song *et al.*[119]
		Lamprotula	*Lamprotula fibrosa*	Sun and Tong[17]
Gastropods	Calliostomatidae	*Calliostoma*	*C. zizyphinum*	Cartwright and Checa[9]
	Haliotidae	*Haliotis* (abalone)	*Haliotis asinina*	Cartwright and Checa[9]
			Haliotis fulgens (green abalone)	Lin and Meyers;[91] Meyers *et al.*[25,86]
			Haliotis genus	Heinemann *et al.*[43]
			Haliotis iris	Song *et al.*[35,36]
			Haliotis laevigata (greenlip abalone)	Blank *et al.*;[84] Heinemann *et al.*[43]
			Haliotis rufescens (red abalone)	Barthelat *et al.*;[31,48] Bezares *et al.*;[109,120] Fleischli *et al.*;[10] Fritz *et al.*;[87] Li *et al.*;[38,54] Lin *et al.*[68] Fig. 3, Fig. 8; Lin and Meyers;[91,121] Katti *et al.*;[41,50] Menig *et al.*;[46] Meyers *et al.*;[32,26,86] Mohanty *et al.*;[51] Schäffer *et al.*;[33] Verma *et al.*;[95] Wang *et al.*;[5]Yao *et al.*;[102] Yourdkhani *et al.*;[8] Zaremba *et al.*[2]
			unkonwn	Meyers and Chawla[97]
	Pleurotomariidae	*Perotrochus*	*Perotrochus caledonicus*	Checa *et al.*[94]
	Strombidae	*Strombus*	*Strombus gigas*	Menig *et al.*[122]
	Trochidae	*Gibbula*	*Gibbula pennanti*	Cartwright and Checa[9]
			Gibbula umbilicalis	Cartwright and Checa[9]
		Trochus	*Trochus niloticus* (top shell)	Bruet *et al.*;[49] Currey[45]
	Turbinidae	*Bolma*	*Bolma rugosa*	Cartwright and Checa[9]
		Turbo	*Turbo marmoratus*	Chateigner *et al.*;[83] Currey[45]
Cephalopods	Nautilidae	*Nautilus*	*Nautilus pompilius*	Currey[45]
Monoplacophora	Neopilinidae	*Veleropilina*	*Veleropilina zografi*	Checa *et al.*[94]

2 Hierarchical structure

Nacre has a complex hierarchical architecture that spans multiple length scales from the nanoscale to the macroscale,[6,8,12,22,25,26] as shown in Fig. 3.[26] It is an important characteristic of structural materials similarly found in bone, teeth and other tissues.[27] There are some noticeable differences when examining varying species of nacre, for example the thickness of the tiles in the abalone nacre is approximately 0.5 μm, while it is around 0.3 μm for bivalve nacre.[32]

Several models have been proposed to explain why nacre achieves its strength owing to the microstructure of "mineral tablets embedded in a thin organic matrix".[5,40,47,74–80]

In the following, we present the nacre structure, from the mesoscale to the nanoscale: two different columnar and sheet nacre structures in gastropods and bivalves, respectively; mineral bridges which represent the continuation of mineral growth along the *c*-axis from a preceding layer of tiles; different crystal formation and growth in gastropods and bivalves; aragonite tablets consisting of 3–10 nm polygonal nanograins; and inter-tile toughening

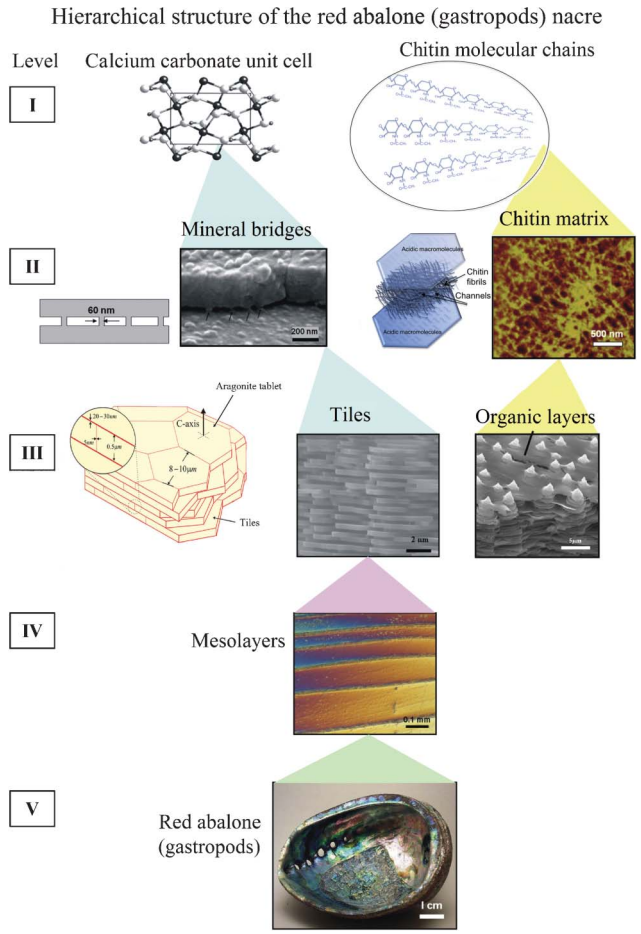

Fig. 3 Hierarchical structure (5 levels) of the red abalone (gastropod) nacre from nano, to micro, to meso, to structural length scales.[26]

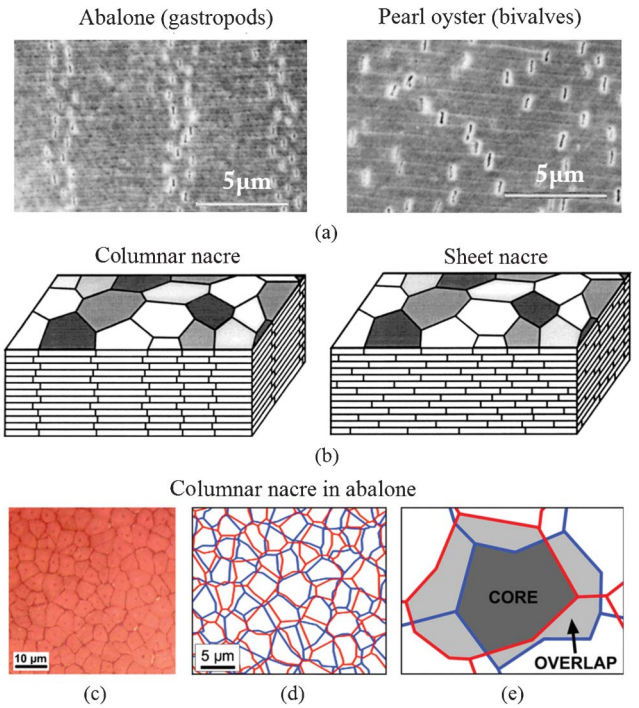

Fig. 4 SEM images of deformation bands by tensile testing of (a) abalone (gastropods), showing four vertical dilatation bands and pearl oyster (bivalves), where the separations are randomly dispersed, and (b) schematic illustrations of columnar nacre/abalone and sheet nacre/pearl oyster. Polygonal aragonite tablets are adhered into a lamellar structure by a thin organic interlayer. In columnar nacre, the intertablet boundaries are correlated into a tessellated arrangement;[5] (c) optical image of the cleaved surface shows a Voronoi like tiling of the tablets within one layer in red abalone nacre viewed from the top; (d) reconstitution of the arrangement of the tablets from one layer to the next, and (e) core and overlap areas in the tablet arrangements.[48]

mechanisms including plastic microbuckling, crack deflection, interlocking, nano-asperities and representative models.

2.1 Columnar and sheet structure

The precise geometric arrangement of the tiles is one of the important reasons for the robust mechanical behavior of nacre.[45] There are two different mineralization types of nacre: *Gibbula umbilicalis* (gastropods) and *Nucula nitidosa* (bivalves) on the microscale, as shown in Fig. 4a.[5] Nacres are "columnar nacre" or "sheet nacre", depending on the stacking mode of the tablets (Fig. 4b). Columnar nacre has tablets of a rather uniform size with coinciding centers that determine the nucleation site of the overlying tablet, while in sheet nacre deposition takes place over most of the inner surface of the shell, and the tablets are stacked in a "brick wall" pattern, spanning the interface between the underlying tablets.[81–83] Generally, columnar nacre is found in gastropods, whereas sheet nacre occurs more in bivalves.[45] In columnar nacre, viewed from the top, the polygonal tablets from neighboring layers overlap in such a manner that the inter-tablet boundaries form tessellated bands perpendicular to the lamellae boundaries, shown in Fig. 4c–e.[48] While in sheet nacre, the inter-tablet boundaries are distributed randomly. The overlap region in columnar nacre covers around 1/3 of the area of a tablet, whereas in sheet nacre no distinction can be made between the core and overlap areas.[8,48] In columnar nacre, the distinction between the core and the overlap region is important, because the stresses experienced by these two regions are different.[31]

The tablets in nacre are often described and modeled as being flat on the microscale; it was actually observed that the interfaces between the tablets show significant waviness, contributing to energy dissipation.[48]

2.2 Mineral bridges

The existence of mineral bridges connecting individual tablets was first demonstrated by Schäffer *et al.*[33] and later confirmed by others. They proposed that the mineral bridges improve the mechanical properties of the organic matrix layers and prevent crack extension in nacre.[9,31,35–37,68]

These bridges represent the continuation of mineral growth along the *c*-axis from a preceding layer of tiles. They protrude through the growth-arresting layers of proteins, creating sites on the covering organic layer where mineralization can continue, as shown in Fig. 5.[68] To directly observe the mineral bridges between individual tablets, nacre was fractured in tension parallel to the direction of growth.[35,36] In Fig. 5a, arrows mark the locations of the remaining mineral bridges, while a gap between tile layers can be clearly seen to exist in the absence of the organic matrix. Fig. 5b provides further evidence of mineral

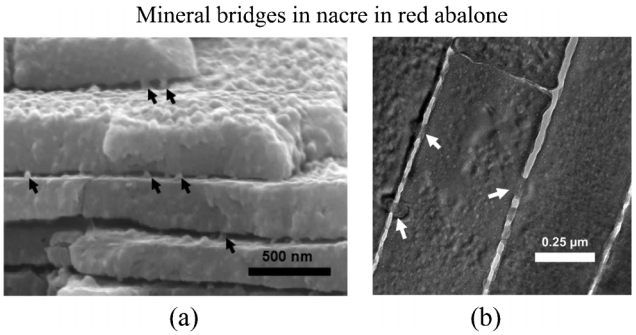

Fig. 5 TEM images of the red abalone nacre cross-section showing (a) mineral bridges between tile interfaces and (b) mineral bridges between tablets of neighboring layers shown by arrows.[79] These mineral bridges are also found in bivalves.

bridge formation and the aragonite surrounding individual mineral bridges seems to have semicircular bands emanating from the bridge. It has been suggested that this corresponds to a higher degree of protein absorption during the process of mineral bridge formation.[79]

2.3 Crystal formation and growth

The growth surface of the nacre plays a critical role in determining its mechanical properties and is a powerful crack deflector.[32] During the growth of the shells, the prismatic layer is deposited first and the nacre is added as the shell thickness increases with time.[29] The aragonite tablets appear as 'stacks of coins', where the next layer of tablets is already nucleated without the underlying layers being confluent, then tablets grow in the horizontal direction until the layer is closed.[84] On the formation mechanism of individual tablets, there are three important hypotheses, being (1) single crystal growth, (2) a coherent aggregation of nanograins, and (3) phase transformation from amorphous calcium carbonate (ACC) or metastable vaterite to stable aragonite.[85]

Fig. 6 shows the mechanism of growth of nacreous tiles by the formation of mineral bridges in gastropods; the organic layer is permeable to calcium and carbonate ions, which nourish lateral growth, as periodic secretion and deposition of the organic intertile membranes restricts their flux to the lateral growth surfaces.[86] Arrows A designate the organic interlayer imaged by scanning electron microscopy (SEM) and arrow B designates the lateral boundary of the tile.

It has been confirmed that the growth of the aragonite component of the composite occurs by the successive nucleation of aragonite crystals and their arrest by means of a protein-mediated mechanism; it takes place in the "Christmas-tree pattern".[87] For bivalves, it usually has a rectangular, hexagonal or rounded shape when growing, but when it meets adjacent tablets and stops growing the crystal shape becomes polygonal.[88] Fig. 7 shows the two types of nacre structure with different formation methods. There are significant differences in the arrangement of the $CaCO_3$ crystals, the axes along which these crystals are arranged (the crystal textures), and the way in which they are deposited.[9,87,89–93] When the growth surface of nacre is viewed on the mesoscale, piles of tablets are seen to give rise to a landscape of columns in gastropods, while steps or terraces of tablets form arrangements of spirals, labyrinths and target patterns in bivalves.[9,94]

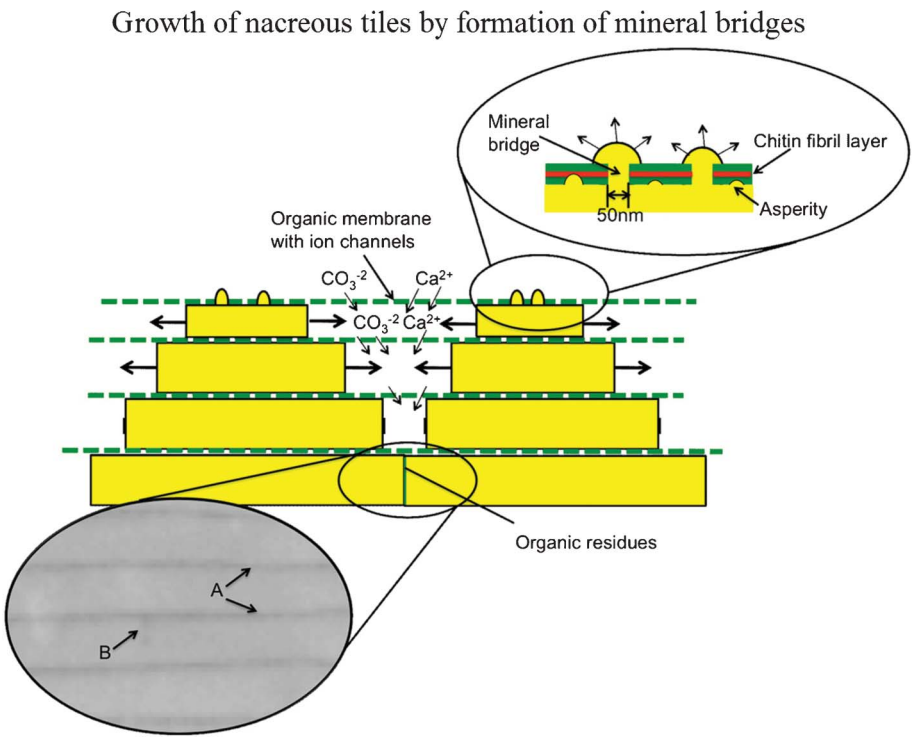

Fig. 6 Mechanism of growth of nacreous tiles in abalone by formation of mineral bridges; the organic layer is permeable to calcium and carbonate ions, which nourish lateral growth as periodic secretion and deposition of the organic intertile membranes restricts their flux to the lateral growth surfaces. Arrows A designate the organic interlayer imaged by SEM; arrow B designates the lateral boundary of the tile.[86]

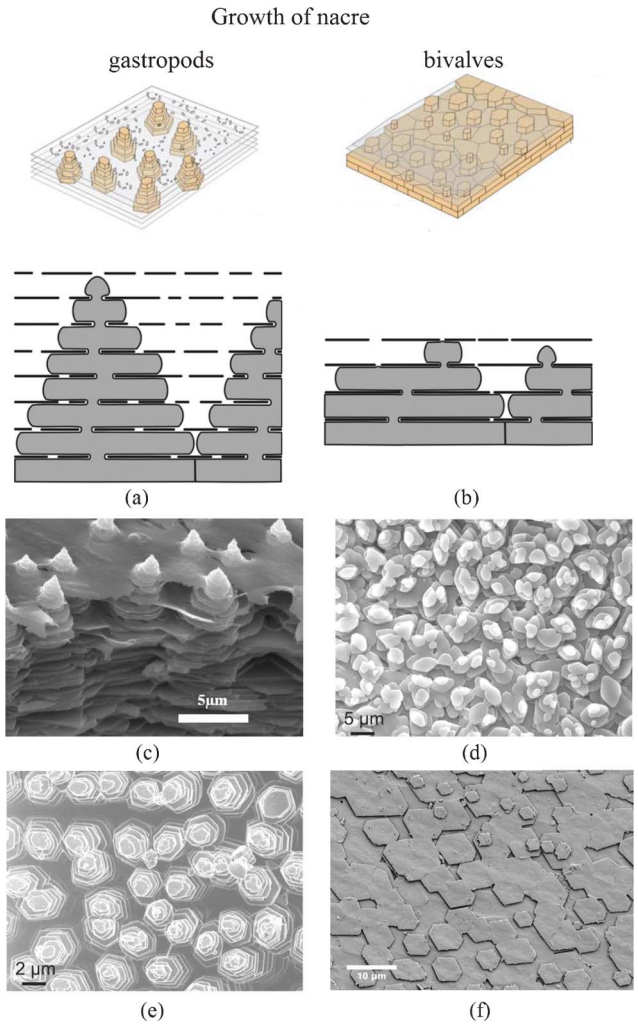

Fig. 7 Schematic showing the growth of nacre in (a) gastropods and (b) bivalves.[94,114] In the normal bivalve situation, small and scarce pores lead to 3 stacked nacre plates (in this example); in the gastropod model, pores are much more frequent and bigger in size, which allows plates to create other plates in the interlamellar space above. This results in up to 7 stacked plates. (c) SEM images of the "Christmas tree" pattern observed on the growth surface of steady state tiled aragonite gastropod red abalone nacre;[25] (d) and (e) SEM image of marginal nacre in the bivalve *Nucula sulcata*, where tablets grow in low towers, and towered nacre in the gastropod *Osilinus lineatus*, respectively;[37] (f) SEM image of the forming layers of bivalves *Atrina rigida*.[88]

2.4 Polygonal nanograins

On the nanoscale, the polygonal nanograins were observed on the aragonite tablets, which are the basic building blocks in nacre.[54] High-resolution transmission electron microscopy (TEM) (top view) of a tablet shows nanograins of about 3–10 nm in size, shown in Fig. 8a,[31] providing a ductile nature to such microstructures.[33] Such deformability of the aragonite tablets is relevant for nacre's high fracture toughness.

Based on *in situ* atomic force microscopy (AFM), observations of the nanogranular texture of the aragonite tablets during mechanical deformation, nanograin rotation and deformation occur, facilitated by the existence of the biopolymer spacing between the nanograins, which will contribute to energy dissipation in nacre, shown in Fig. 8b.[38,39] The water present at the nanograin interfaces may facilitate the viscoelastic features in nacre.[95]

2.5 Inter-tile toughening mechanism

One of the outstanding features of nacre is its high toughness. Therefore, the toughening mechanisms and their guide to materials synthesis are of interest.[96] Currey[45] mentioned several toughening mechanisms: plastic deformation ahead of the crack tip, crack deflection, crack blunting, and tablet pullout. Earlier research on nacre's toughening mechanisms focused mostly on crack deflection,[13,97] fiber (aragonite platelet) pull out,[96] and organic matrix bridging;[98] recent observations on the inter-tile toughening mechanism focused dilatation band formation[5,48] and nanograin rotation.[38] However, it is reported that the many orders of magnitude increase in toughness cannot only be caused by tortuosity, which is one of the toughening mechanisms proposed by Sarikaya.[99] (see also Meyers *et al.*[32]). Additional toughening mechanisms, such as sliding of $CaCO_3$ layers and organic ligament formation, were thought to operate and were analyzed by Lin and Meyers.[91]

Fig. 9 shows a plastic microbuckling event observed along the mesolayers, which is a mechanism for decreasing the overall strain energy, and was observed in a significant fraction of the specimens.[46] The coordinated sliding of layer segments of the same approximate length by shear strain produces an overall rotation of the specimen in the region with a decrease in length.[25] The angle α in Fig. 9 was measured and found to be approximately 35°. The ideal angle, which facilitates microbuckling, is about 45°, which means nacre exhibits a low value of kinking failure stress. The angle θ (rotation inside the kink band) is approximately 25°, determined by the interlamellar sliding.[46] The rotation θ in kinking is limited by the maximum shear strain; if θ were to exceed a certain value, fracture along the sliding interfaces would occur.

A significant mechanism of toughening is crack deflection on both the meso- and microscale, shown in Fig. 10a.[97] Fig. 10b shows cracks that are deflected at each soft layer. The effect of the viscoelastic glue (organic material) is to provide a crack-deflection layer, so that cracks have difficulty propagating through the composite of layers of calcium carbonate.[32] The toughness of this laminated composite is vastly superior to that of a monolithic material, in which the crack would be able to propagate freely, without barriers.[97] The two levels of the structure presented in Fig. 10 can be seen engaging in this mechanism: (a) mesolayers provide crack deflection, (b) on a smaller scale the tile layers force cracks into a tortuous path.[79]

The interlocking of the tablets, first reported by Katti *et al.*,[41] is shown in Fig. 11a. It appears that when two tablets are stacked above one another, rotated by a small angle relative to each other, the upper tablet with organic material is wrapped around and penetrates into the lower tablet to form the interlocks (Fig. 11b). When load is applied parallel to the tablets, the 20 nm-thick organic layer surrounding the tablet provides the deformable medium, producing additional deformation before failure of the aragonite interlock (Fig. 11c). The interlocks provide a large contribution to the strength of nacre.

Evans *et al.*[40] and Wang *et al.*[5] proposed a toughening mechanism: those nano-asperities on the tablets are responsible

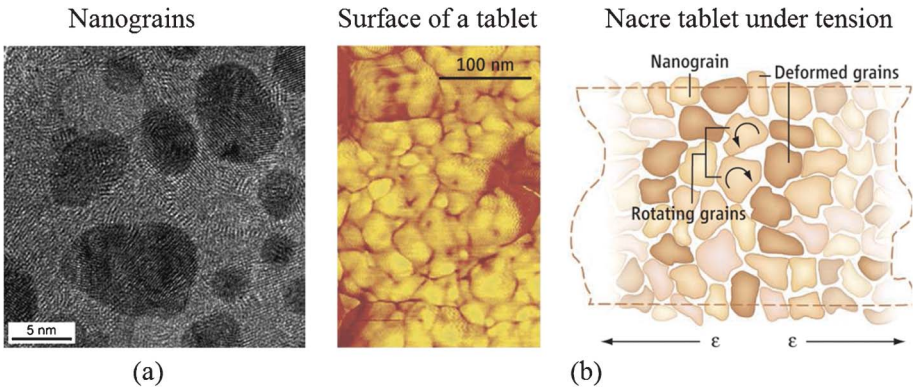

Fig. 8 (a) High-resolution TEM (face-on view) of a tablet from the nacreous layer of a red abalone specimen showing nanograins of about 3–10 nm in size;[31] (b) (left) AFM image of surface nanograins on an individual nacre platelet from California red abalone and (right) schematic of nanograin rotation under tension.[38,39]

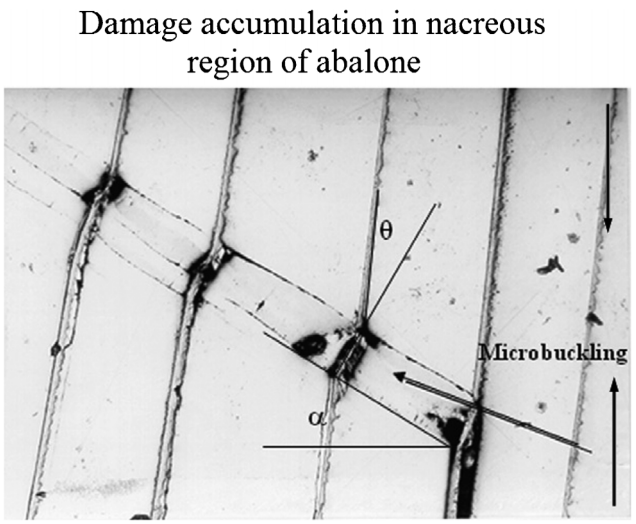

Fig. 9 Mechanisms of damage accumulation in the nacreous region of abalone through plastic microbuckling.[46]

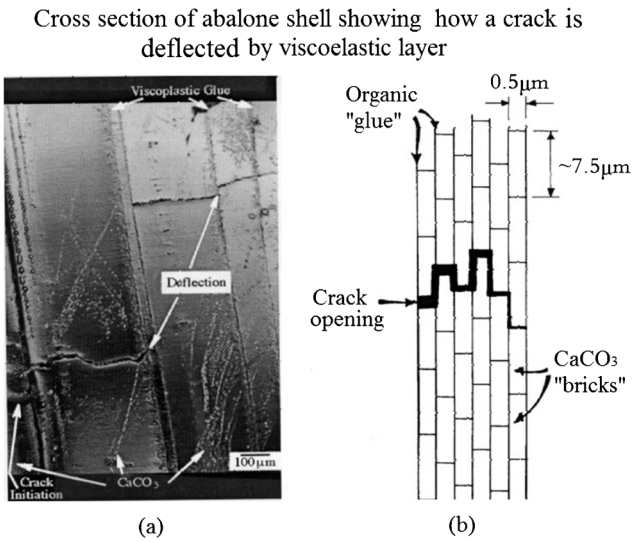

Fig. 10 (a) Cross-section of abalone shell showing how a crack, starting at the left, is deflected by the viscoplastic layer between calcium carbonate lamellae; (b) schematic drawing showing the arrangement of calcium carbonate in nacre, forming a miniature "brick and mortar" structure.[97]

for the mechanical strength. The number of asperities seen in Fig. 12a exceeds considerably the values for the bridges calculated herein.[5,68] These images affirm that the asperities on the upper aragonite tablet interpose with those on the lower tablet. Fig. 12b shows that the fibrils can stretch out to a remarkable length, equivalent to a strain of 150%, without becoming detached from the calcium carbonate.[13] Fig. 12c (i)–(iv) present schematics of the various inter-tile toughening theories.[79] It is hypothesized that the asperities are the principal source of shear resistance, shown in Fig. 12c (i). Hence, plate fractures will not happen internally. Plate fractures also cause deformation delocalization. The proteins consisting of beta-pleated sheets folded into cross-linked polymer-like glue would adhere to the tiles and provide toughness through the many sacrificial bonds between proteins.[98] The model for it, represented in Fig. 12c (ii), shows the viscoelastic glue model according to which the tensile strength is the result of the stretching of molecular chains whose ends are attached to the surfaces of adjacent tiles.[79] At the onset of plastic deformation, broken mineral bridges may play a role in forming the asperities

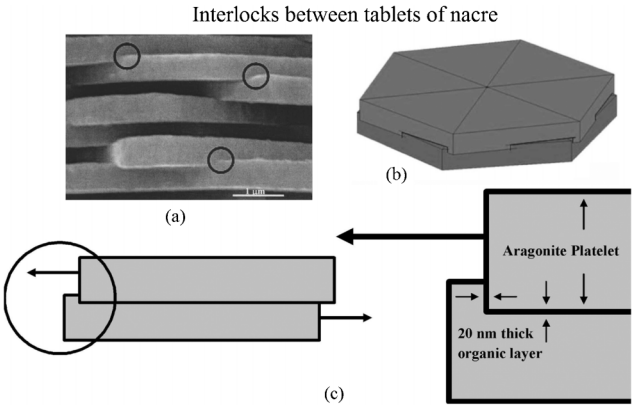

Fig. 11 (a) SEM image of nacre from red abalone showing the presence of interlocks, indicated by circles; (b) schematic illustration showing interlocks between platelets of nacre, showing that rotation of layers of platelets is essential for the formation of platelet interlocks. (c) Schematic illustration showing the mechanism of loading through a cross-section cut across platelets and through the interlocks.[41]

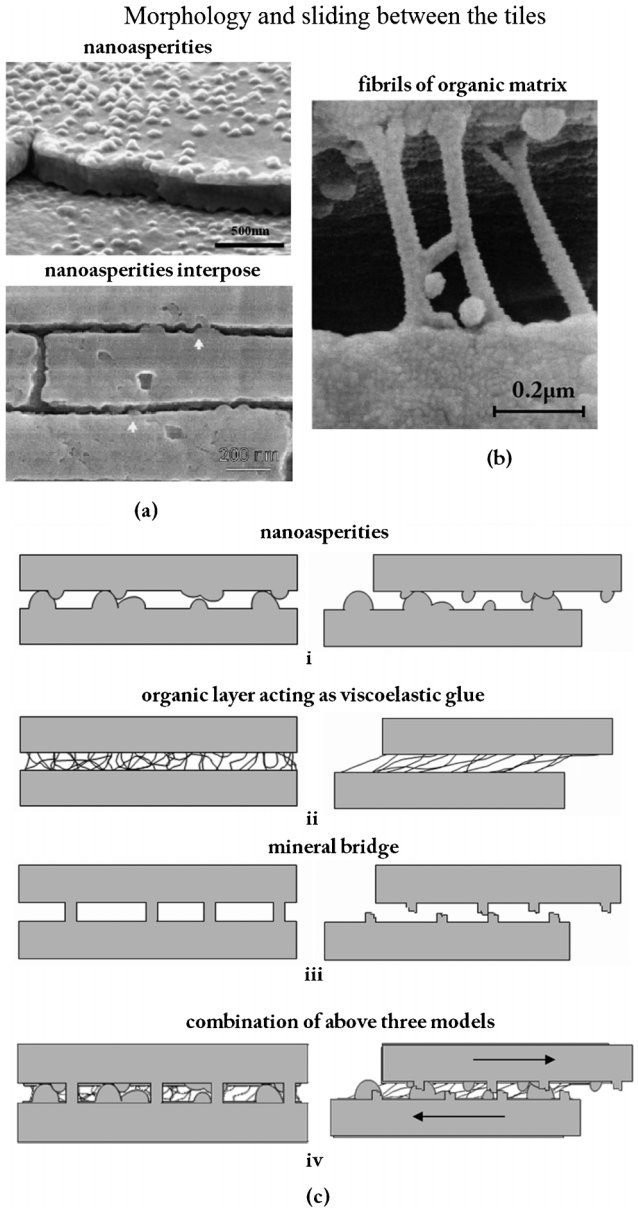

Fig. 12 (a) Asperities (a fraction of which are remnants of mineral bridges);[68] cross section of abalone nacre showing the detailed structure at the lamellae boundaries, where arrows highlight locations where the nanoasperities interpose;[5] (b) fibrils of the organic matrix bridging a delamination crack. Note the large extension and 'splayed-out' anchorage points.[13] (c) Different models for sliding between tiles:[79] (i) inter-tile layer formed by asperities; (ii) organic layer acting as viscoelastic glue; (iii) mineral bridges; (iv) combination of the three mechanisms.

that subsequently resist shear,[25,35,36,100] as in the model shown in Fig. 12c (iii). It is suggested here that the true mechanism of toughening is the combination of the above three models in a synergetic and harmonious collaboration, shown in Fig. 12c (iv).[79] Lin and Meyers[91] suggested that there are two principal mechanisms of failure when tension is applied parallel to the tile direction: tensile fracture of the tile and sliding along the tile surfaces (including breaking of the nanoscale bridges, friction produced by asperities and stretching of organic bonds). And it was deduced that the layered structure of the abalone shell provides anisotropy of mechanical strength, which increases the toughness in a significant manner by increasing the resistance to crack propagation perpendicular to the surface and decreasing it correspondingly parallel to it.[26]

In addition, some other microstructural features were found in nacre: the Voronoi arrangement of tablets in each tile,[101] screw dislocations with unique tessellated zigzag morphology[102] and interconnected layer-to-layer spiral structures[39] may all play a role in the biomechanical functionality.

3 Mechanical properties

Currey[45] was the first to perform measurements of the mechanical properties of nacre from a variety of bivalves, gastropods and cephalopods. He suggested that the tablet geometry and arrangement is optimized for the mechanical properties and energy absorption. This was followed by Jackson *et al.*[13] who studied nacre from the shell of a bivalve mollusk, *Pinctada*, and found that the water absorbed in the organic matrix of nacre plays a significant role in its mechanical response. Following the improvement in precision and diversification of measurement techniques, more in-depth understanding about the mechanical properties of nacre has been acquired. Experimental results reveal that the mechanical properties of nacre, especially high fracture toughness, exist because of its structure.[103]

In the following, we present the mechanical properties of nacre, which include the microscale to the nanoscale: tensile, compressive, shear, micro-scratch and tribological behaviors, nanoindentation properties and modulus mapping.

3.1 Micro-mechanical properties

Fig. 13 summarizes the compressive and ultimate tensile strengths of nacre with respect to various loading directions.[32] The compressive strengths are larger than the tensile strengths in both the perpendicular and parallel directions. Mechanical properties of various nacres are shown in Table 2.

Fig. 14a and b show the tensile and shear behavior of nacre under both dry (ambient conditions) and hydrated conditions (soaked in water), showing some ductility on the macroscale.[48,104] The tensile stress–strain curves are shown in

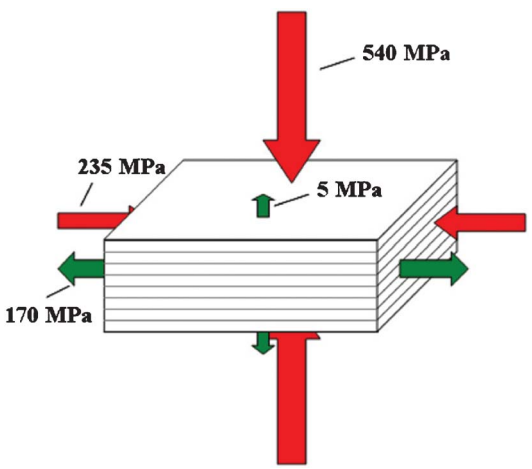

Fig. 13 Compressive and ultimate tensile strengths of nacre under different loading directions.[32]

Table 2 Mechanical properties of nacre

Material	Elastic modulus (GPa)	Hardness (GPa)	Tensile strength (MPa)	Fracture toughness (MPa $\sqrt{m}$)	Compressive strength (MPa)	Shear strength (MPa)	References
Pinctada (Pearl oysters)	70 (D, PA),[a] 60 (W, PA),[a] 73 (D, PE),[a] 64 (W, PE),[a] 81(D,PA),[a] 77(D, PE)[a]		170 (D, PA),[b] 140 (W, PA)[b]	3.7–5 (D, PA),[a] 5 (W, PA),[a] 3.3–4.6 (D, PE),[a] 3.7–4.5 (W, PE)[a]			Jackson *et al.*[13] Wang *et al.*[5]
Pinctada maxima	54.4–62.5 (D, PE)[f]						Stempflé *et al.*[116]
Pinctada sp.			56 (D, PA)[b]				Currey[45]
Pinctada margaritifera			87–106 (D, PA)[b]				Currey[45]
Hyria ligatus			79 (D, PA)[b]				Currey[45]
Anodonta cygnea			35 (D, PA)[b]				Currey[45]
Modiolus modiolus			56 (D, PA)[b]				Currey[45]
Atrina vexillum			86 (D, PA)[b]				Currey[45]
Trochus niloticus			85 (D, PA)[b]				Currey[45]
	114–143 (W, PE),[f] 101–126 (F, PE)[f]	3.6–8.7 (W, PE),[f] 9.7–11.4 (F, PE)[f]					Bruet *et al.*[49]
	70–100 (F, PE)[f]	5.41, 4.89 (F, PE)[f]					Villarreal[123]
Turbo marmoratus			116 (D, PA)[b]				Currey[45]
Lamprotula fibrosa	59.6 (D, PE)[f]	3.42 (D, PE)[f]		6.8 (D, PE)[f]			Sun and Tong[17]
Perna canaliculus (green mussel)	60.9 (D, PE),[f] 61.8–64.7 (W, PE)[f]	4.5 (D, PE),[f] 4.1 (W, PE),[f] 2.55 (D, PE),[g] 2.7–2.75(W, PE),[g] 1.5–2.5 (PE)[h]					Leung and Sinha[106]
	147 (D, PE)[f]						Moshe-Drezner *et al.*[110]
Nautilus pompilius			78 (D, PA)[b]				Currey[45]
Haliotis rufescens (red abalone)				7 (D, PE)[a]			Sarikaya *et al.*;[14] Yasrebi *et al.*[15]
				9(D, PE)[a]			Gunnison *et al.*[16]
			5 (PE)[b]		235 (PA),[c] 540 (PE),[c] 548 (PA),[d] 735 (PE)[d]	30 (PA)[e]	Menig *et al.*[46]
			3 (PE)[b]		250 (PE)[c]		Lin[79]
	90 (D, PA),[b] 70 (W, PA),[b] 14 (D, PA),[e] 10 (W, PA)[e]						Barthelat *et al.*[48]
	79 (D, PE)[f]	7.5(D, PE)[f]					Barthelat *et al.*[31]
	66 (D, PA),[a] 69 (D, PE)[a]						Wang *et al.*[5]
			65 (F, PA)[b]			36.9 (F, PA)[e]	Lin and Meyers[121]
	60–80 (D, PE)[f]	2–4 (D, PE)[f]					Li *et al.*[54]
	14.85–113.74 (PE),[f] 40.95–56.71 (PE)[f]	0.69–19.32 (PE),[f] 1.32–3.21 (PE)[f]					Katti *et al.*[50]
			10 (F, PE)[b]		300–500 (F, PE)[c]		Meyers *et al.*[25]
	70–114 (D, PE)[f]						Bezares *et al.*[109]

Testing methods:[a] three-point bending testing; [b] tensile testing; [c] quasi-static compression; [d] dynamic compression; [e] shear testing; [f] nanoindentation testing; [g] Vickers hardness testing; [h] scratch testing. Materials status: D- Dry, W- Wet, F- fresh. Loading direction: PA- parallel to the surface plane; PE- perpendicular to the tablet lamella

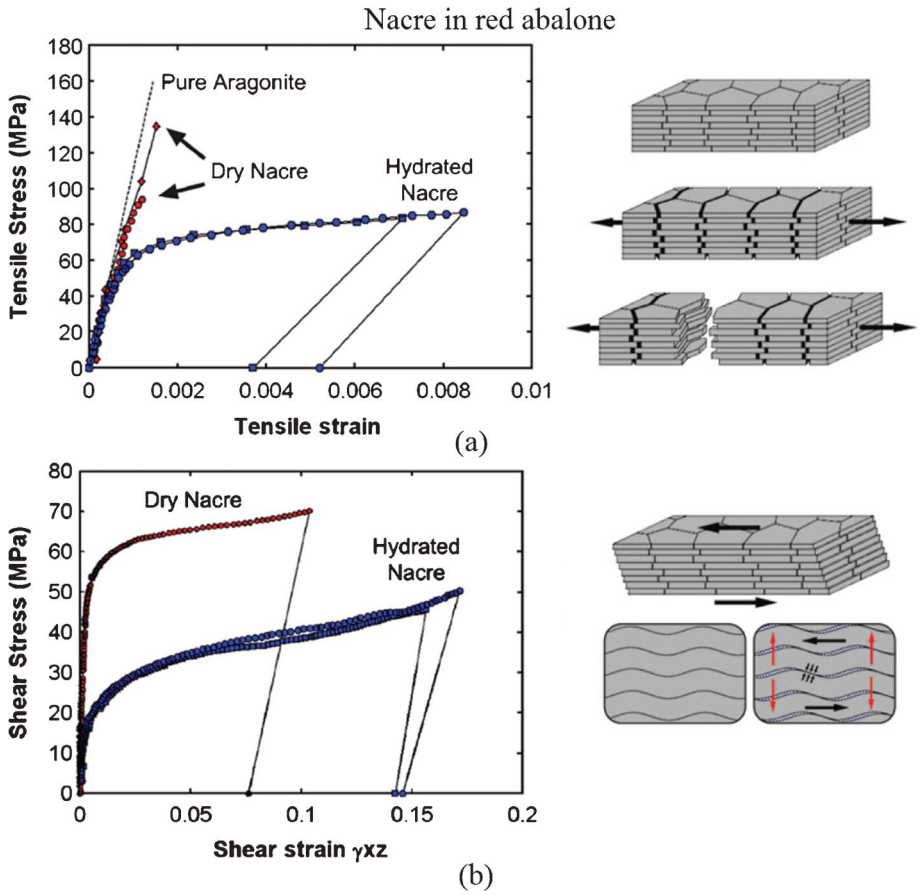

Fig. 14 (a) Tensile and (b) shear stress–strain curves for nacre in red abalone and a schematic of lamellar tile structures showing associated deformation modes. Tablet waviness generates resistance to sliding, accompanied by lateral expansion (vertical arrows).[48,104]

Fig. 14a; the behavior of dry nacre is similar to that of pure aragonite and failed in a brittle fashion. It showed that dehydrated nacre loses its strength. On the other hand, it demonstrated that the organic materials (5 wt%) are essential to nacre. After an initial linear response, similar to dry nacre, hydrated nacre showed a region of larger inelastic strain, starting at a stress of 70 MPa. While this mechanism can easily be envisioned as simple shear (Fig. 14b), it is less obvious in tension (Fig. 14a), because tablet sliding only occurs in the tablet overlap areas. Jackson *et al.*[13] concluded that water affects the elastic modulus and tensile strength by reducing the shear modulus and shear strength of the organic matrix, and the toughness is enhanced by water, which plasticizes the organic matrix, resulting in greater crack blunting and deflection abilities.

Fig. 15 shows the compression stress–strain curves for abalone nacre, representing interlamellar shear, measured both in monotonic loading and with loading–unloading loops.[5] The insert indicates that the lamella boundaries are orientated at 45° to the loading axis; the unloading–reloading measurements reveal hysteresis, indicative of internal friction and viscoelasticity.

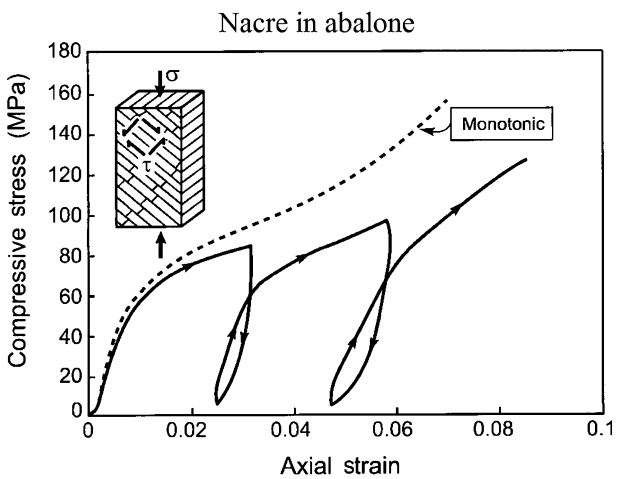

Fig. 15 Compression stress–strain curves for nacre in abalone, representing interlamellar shear, measured both in monotonic loading and with loading–unloading loops. The insert indicates that the lamellae boundaries are orientated at 45° to the loading axis.[5]

Because Weibull distribution is generally a better choice for the description of strength data for ceramics, Menig *et al.*[46] measured the compressive strength of red abalone, and found a considerable variation in results based on it. Fig. 16a and b show Weibull analysis of abalone nacre in quasi-static and dynamic compressive loading, with loading parallel and perpendicular to the layered structure.[46] m is the Weibull shape parameter or Weibull modulus, which is an inverse measure of the distribution width; that is, a high value of m corresponds to a narrow

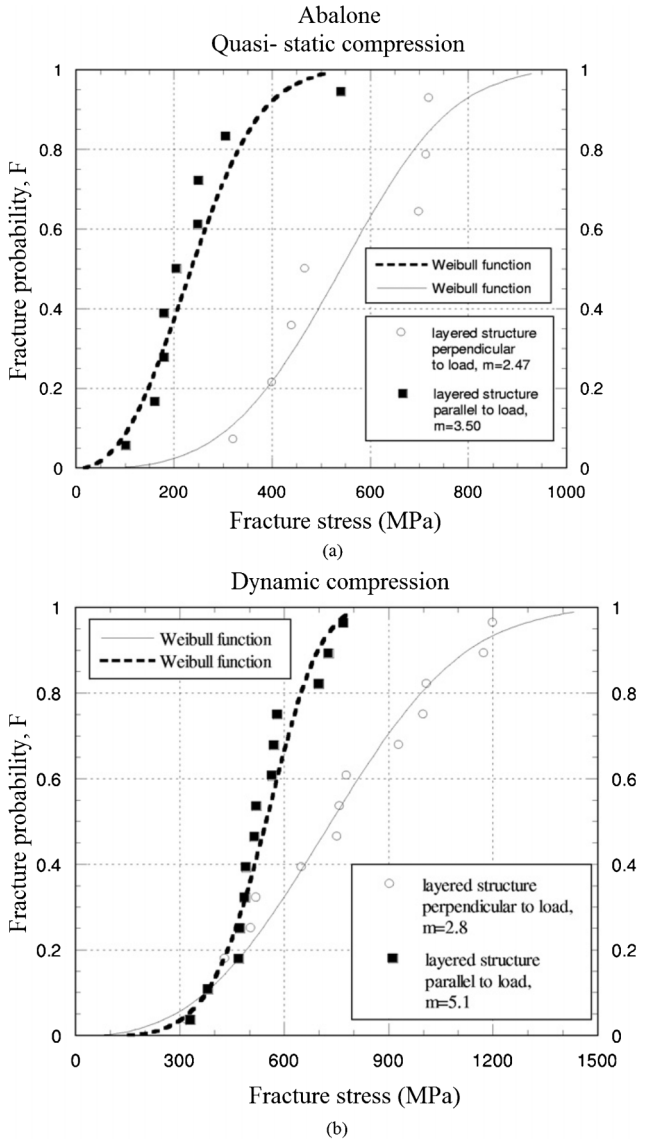

Fig. 16 Weibull plots of abalone nacre in abalone under (a) quasi-static, and (b) dynamic compressive loading.[46]

distribution.[105] With failure probabilities of 50%, the abalone nacre is stronger with layers perpendicular to the loading direction. The dynamic strength of abalone is approximately 50% higher than its quasi-static strength. Comparing to compressive strength, *m* was acquired by tension perpendicular to the direction of the layers,[25] and its value (1.6) is similar to that in the compressive test (2.47); in contrast the strength is dramatically smaller (5 MPa) than that in the compressive test (540 MPa).

For investigating the role of water content in the organic matrix and the scratch/nanoindentation hardness on the toughness mechanisms, micro-scratch tests and indentation tests were performed on the soaked and dry surfaces of nacre of green mussel shells.[106] Both sets of experiments showed a decrease in hardness as a result of hydration. The data suggest that nacre toughness is affected by hydration.

Friction and wear behavior of sheet nacre has been studied in dry and wet environments.[107,108] It was found that the coefficient of friction is rather high under dry conditions (0.45), and even higher under wet conditions (0.78).[107] The environment influences the wear mechanisms of nacre by means of various physicochemical interactions on the water-soluble "intracrystalline" organic phase. Friction-induced damage mechanisms involving thermal effects remain largely not understood.[108]

3.2 Nanomechanical properties

The mechanical properties of nacre have been studied using nanoindentation experiments.[49–51] Mohanty *et al.*[51] reported the dynamic nanomechanical behavior of nacre and showed that the aragonite platelets are viscoelastic in nature and can absorb energy.

The value of *E* for polished red abalone nacre samples was found to be between 60 and 80 GPa.[54] It was also reported that there is plastic deformation in the indented region. For *Trochus Niloticus* nacre, the reported values of *E* were between 114 and 143 GPa for freshly cleaved samples and between 101 and 126 GPa for artificial seawater soaked samples.[49] Images of the indents revealed extensive plastic deformation with a clear residual indent and surrounding pile-up. Compared with these values, the *E* value of a single tablet was 79 GPa,[31] which is close to that of monolithic aragonite (81 GPa). The organic phase between the layers of aragonite tablets has been shown to exhibit *E* values between 2.84 and 15 GPa.[31,74] This suggests that the softer interfaces and structure of the tablets have an effect on the overall mechanical properties of nacre.

Typical indent profiles of nacre from red abalone are shown in Fig. 17.[109] Fig. 17a and b show indentation data for dry and hydrated (or wet) nacre, respectively. Fig. 17b shows that the

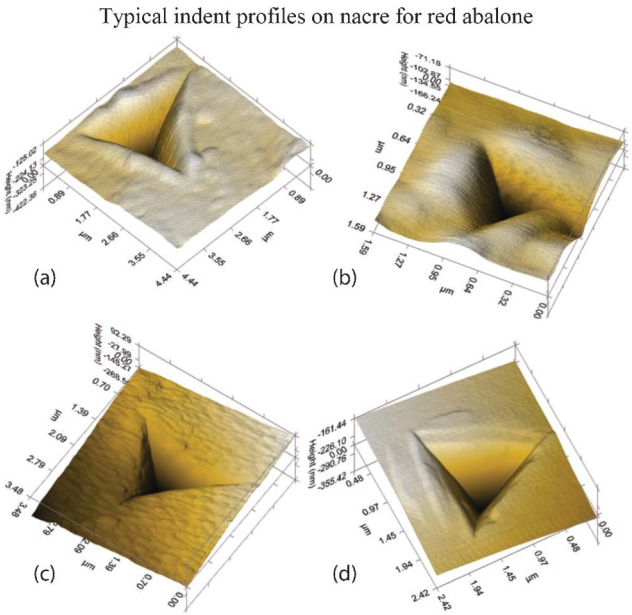

Fig. 17 Typical indent profiles on nacre from red abalone: (a) dry nacre, there are pile-ups around the edges; (b) wet nacre, the blunted appearance of the indentation is related to the compliance of the wet nacre seen from its relatively low modulus; (c) heat treated nacre, the material appears compacted and similar to what happens to sand when it is heated and grains begin to fuse together; and (d) monolithic aragonite, the uneven pile-up indicates anisotropy.[109]

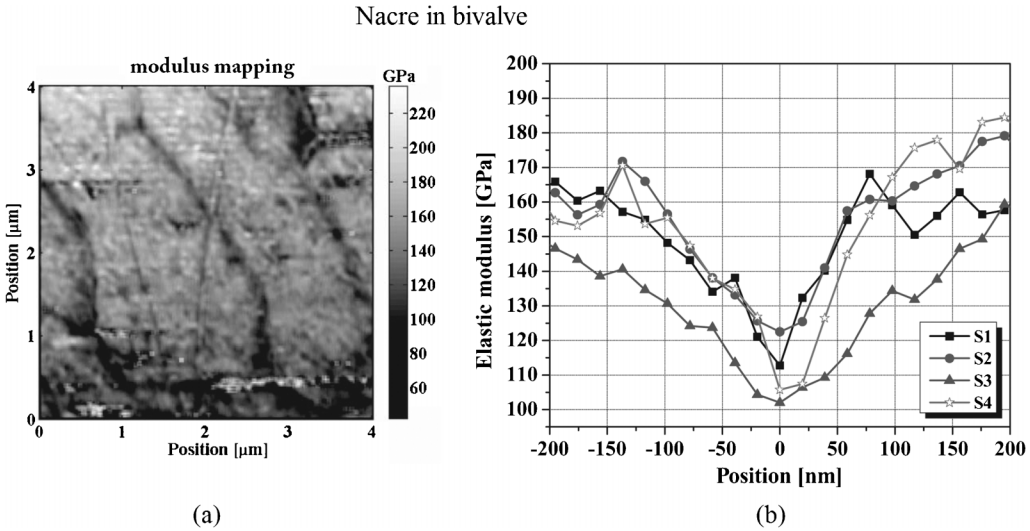

Fig. 18 (a) Map of elastic modulus taken from the nacre layer at a depth of 300 μm beneath the inner surface of the bivalve shells of *Perna canaliculus*; (b) the modulus change across organic–inorganic interfaces.[110]

form of the indentation was different in that the pile-ups are far more "blunted", with a much reduced hardness as compared to dry nacre. Scans of the indentation profiles made on heat treated nacre shown in Fig. 17c do not resemble both the dry and the wet cases. The tiles appeared to have sharp edges and displayed no pile-ups *per se*, and with the concomitant loss in intra-tile protein, nacre behaves as a loosely bound granular material. The indentation profiles on monolithic aragonite displayed anisotropic pile-ups, unlike nacre (Fig. 17d).

A modulus mapping of nacre of *Perna canaliculus* (green mussel), is presented in Fig. 18a.[110] It shows periodic contrast produced by lighter aragonite regions separated by curved darker lines with significantly lower *E*. The change in *E* across organic–inorganic interfaces is shown in Fig. 18b, within a spatial range four times wider than the thickness of the organic layers.

Using force mode AFM, it has been shown that a very large force is required (>5–6 nN) to pull the proteins away from the aragonite, which suggests that the molecular interactions at the organic–inorganic interface in nacre are substantial and may play a significant role in the overall toughness of nacre.[111]

4 Bioinspired structures

Mimicking the nacre hierarchical structure is more complex than other biomimetic structures. Hierarchically-structured materials typically offer control over two degrees of hierarchy: (i) thickness and orientation of the layers and (ii) control of the interfacial properties between layers (roughness, residual stresses).[112] Overall, the mimicking of nacre is mainly focused on (1) structure, including laminated structure, hierarchical structure, brick-like structure, or organic and inorganic multilayered structure (brick-and-mortar structure), (2) manufacturing process, that means mimicking its mineralization process, and (3) components, mimicking its 5 wt% organic with inorganic materials for producing artificial nacre. These design concepts and fabrication methods have been used with various non-metallic materials and polymers for enhancing or improving their original mechanical properties.

A laminated structure of Al-B_4C was produced by Sarikaya and Aksay.[113] They reported that it was five times tougher than monolithic B_4C. Thenceforth the highly organized microarchitecture and extraordinary mechanical response of nacre have inspired scientists to develop synthetic nanocomposite materials mimicking nacre.[12] Table 3 shows some refined ceramic materials that were bioinspired by the structure of nacre. The fracture toughness of biomimetic composite materials approached that of nacre. The bioinspired structures of nacre have also been applied to composite materials,[1,59,62–73] coatings,[55] and films.[18,56–61] Nacre-mimetic paper has been fabricated with lightweight, shape-persistent, excellent and tunable mechanical properties, and heat and fire-shielding capabilities.[61]

Based on fabrication methods, the bioinspired structures can be considered from two different points of view: hierarchical

Table 3 Fracture toughness values for various refined ceramic materials, which were bioinspired by nacre

Bioinspired nacre structural materials	Scale	Fracture toughness (MPa $\sqrt{m}$)	Reference
Al/Al–Si	μm	5.5–10	Deville *et al.*[59]
Al_2O_3/Al–Si	μm	40	Lin *et al.*;[123] Launey *et al.*[72]
Al_2O_3/PMMA[a]	μm	30	Munch *et al.*[69]
Al_2O_3/TiO_2	mm	12	Bueno and Baudín[70]
$SiC/Al_2O_3–Y_2O_3$	mm	14	Zhang and Krstic[63]
Si_3N_4/BN	mm	28	Wang *et al.*[64]

[a] Polymethyl methacrylate (PMMA)

structure (top-down) and self-assembled nanocomposite (bottom-up).[112] Due to the wide range of applications of the biomimetic nacre structure, various fabrication methods have been used. On the nanoscale, as an example, a high-strength and highly transparent nacre-like nanocomposite has been prepared *via* a layer-by-layer assembly technique from poly (vinyl alcohol) (PVA) and Na^+-montmorillonite clay nanosheets, which are strong, flexible, but also highly transparent.[60] The preparation of a "nacre-like" nanocomposite (NC) *via* layer-by-layer (LBL) assembly of the poly (diallyldimethylammonium chloride) polycation (PDDA) is shown in Fig. 19a. The growth profile of the films, characterized with UV-vis spectroscopy and ellipsometry (Fig. 19b), revealed fairly linear growth. The resulting films were found to be strong, flexible, but also highly transparent, which was attributed to the nanoscale dimensions of the inorganic phase (Fig. 19c and 19d) and high orientation of inorganic clay nanosheets of Na^+-montmorillonite (MTM). AFM phase imaging revealed full platelet coverage of the surface resembling that of nacre (Fig. 19e). SEM imaging revealed a high degree of MTM ordering into a well defined lamellar structure (Fig. 19f).

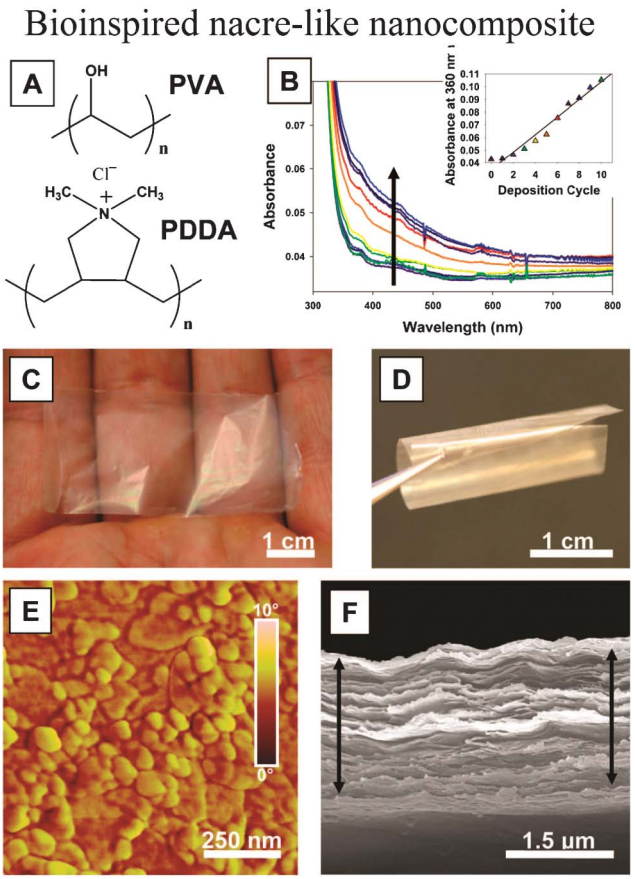

Fig. 19 (a) Structure of PVA and PDDA polymers; (b) UV-vis spectra for the first 10 bilayers of deposition (arrow indicates increasing absorbance, inset represents absorbance at 360 nm as a function of the bilayer); (c, d) optical images of a free-standing film of $(PVA–MTM)_{300}$ showing very high transparency and flexibility; (e) AFM phase image of a single PVA–MTM bilayer; (f) SEM image of the cross section of a 300-bilayer PVA–MTM composite showing its laminar architecture. The films in SEM can be slightly expanded due to separation of the layers resulting from the shearing force of the razor blade used for cutting the test samples.[60]

Upon increasing to the millimeter scale, the design concept of the bioinspired structure of nacre is also suitable for fabrication. Based on the structure of natural nacre, as an example, PMMA tablets exhibiting unique mechanisms were generated.[1] Progressive tablet locking, strain hardening, and spreading of large deformations over large volumes were all achieved in this material. The proposed nacre-like composite material is shown in Fig. 20a. Its main features are borrowed directly from the following design features of natural nacre: stiff and brittle tablets arranged in a columnar fashion with well-defined overlap and core regions, interfaces between the tablets to maintain cohesion

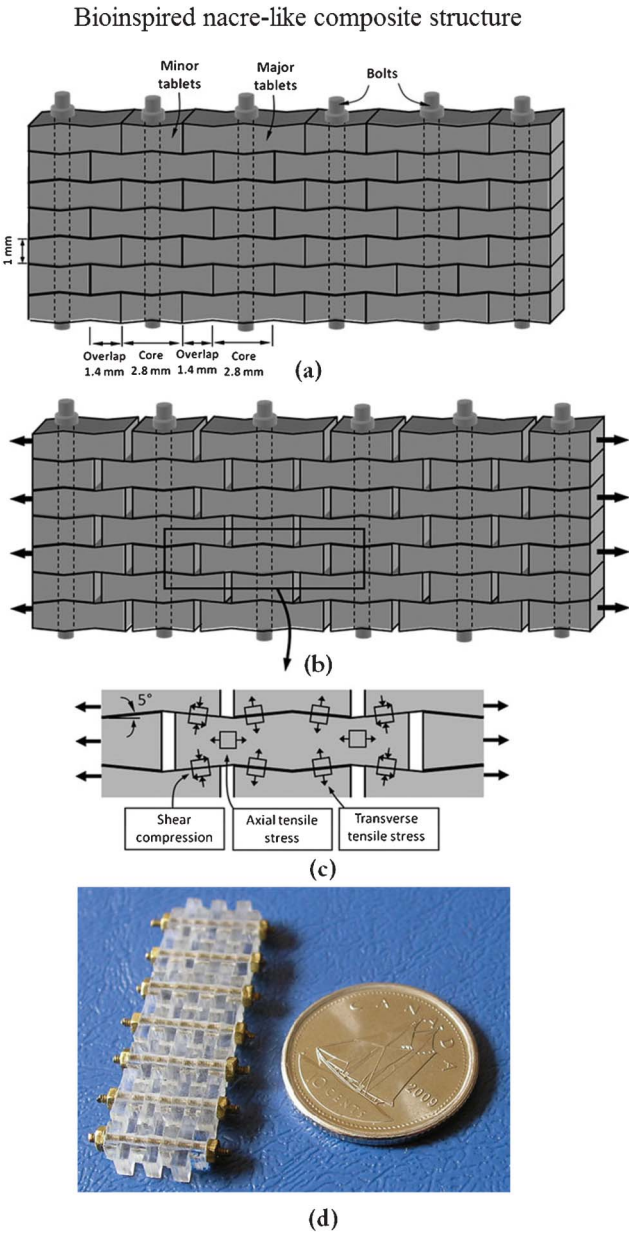

Fig. 20 Overview of the nacre-like composites: (a) schematic with dimensions; (b) tablets under tension slide with progressive locking; (c) some of the stresses involved in progressive locking; (d) actual composite after assembly.[1]

over long sliding distances, and waviness on the tablets to generate strain hardening and spread deformations and reinforcements in the core regions. The anticipated behavior in tension of such a composite is shown in Fig. 20b. The dovetails are critical in generating progressive locking, and the stresses involved in this mechanism are shown in Fig. 20c. The resulting material, shown in Fig. 20d, consisted of seven layers and was composed of eight columns of tablets.

Wang *et al.*[103] summarized various fabrication methods, which have been used in six categories: the conventional method for bulk ceramic materials, freezing casting, layer-by-layer deposition, electrophoretic deposition, mechanical assembly, and chemical self-assembly. Almost all fabrication methods are based on laminate processing.[28] However, the biomimetic structures of nacre have not considered the subtle structures found in nacre, such as tablet waviness, mineral bridges and nanoasperities. With the progress of fabrication methods and theory, the artificial nacre materials will have similar or better mechanical properties in future and can be used in many fields.

Summary

A review of the structure–property relationships in nacre covering the length span from mesoscale features to the nanoscale is presented. Nacre is composed of 95% aragonite ($CaCO_3$) and 5% organic materials. Nacre consists of columnar architectures and sheet tiles, mineral bridges, polygonal nanograins and nanoasperities, showing that nacre is a hierarchical structure material. Aragonite is sandwiched with organic materials and consists of a lamellar bricks-and-mortar microarchitecture with high fracture toughness and strength.

Even though many species of mollusk have a nacreous layer, bivalves and gastropods are the most common and have been the most studied. Data have been presented to understand the mechanisms responsible for good mechanical properties, which include crack deflection, fiber and tablet pull out, organic matrix bridging, dilatation band formation, asperities which resist shear, and nanograin rotation. The mechanical properties of nacre result from its structure and, specifically, from its highly organized micro-architecture with its precise arrangement of mineral platelets. Dry nacre behaves like a monolithic ceramic and fails in a brittle fashion; the elastic modulus of hydrated nacre is lower than that of dry nacre. The water present at the nanograin interfaces also contributes to the viscoelastic nature of nacre.

This research has intrigued materials scientists for decades and has been the subject of biomimetic design. Some examples presented show recent attempts to mimic the structure and properties of nacre using engineered systems.

Acknowledgements

This work was supported by National Natural Science Foundation of China (grant no. 31172144), by the Science & Technology Development Projects of Jilin Province (grant no. 20090147), by the Basic Operation Foundation of Jilin University (grant no. 200903271), Project of the National Twelfth-Five Year Research Program of China (2011BAD20B09-15), and by "Project 985" of Jilin University. We would like to thank Prof. Shunjin Peng for discussion in the materials field.

References

1 F. Barthelat and D. J. Zhu, "A novel biomimetic material duplicating the structure and mechanics of natural nacre", *J. Mater. Res.*, 2011, **26**, 1203–1215.
2 C. M. Zaremba, A. M. Belcher, M. Fritz, Y. Li, S. Mann, P. K. Hansma, D. E. Morse, J. S. Speck and G. D. Stucky, "Critical transitions in the biofabrication of abalone shells and flat pearls", *Chem. Mater.*, 1996, **8**, 679–690.
3 J. H. E. Cartwright, A. G. Checa, B. Escribano and C. I. Sainz-Díaz, "Spiral and target patterns in bivalve nacre manifest a natural excitable medium from layer growth of a biological liquid crystal", *Proc. Natl. Acad. Sci. U. S. A.*, 2009, **106**, 10499–10504.
4 M. Lopes-lima, A. Rocha, F. Goncxalves, J. Andrade and J. Machado, "Microstructural characterization of inner shell layers in the freshwater bivalve *Anodonta Cygnea*", *J. Shellfish Res.*, 2010, **29**, 969–973.
5 R. Z. Wang, Z. Suo, A. G. Evans, N. Yao and I. A. Aksay, "Deformation mechanisms in nacre", *J. Mater. Res.*, 2001, **16**, 2485–2493.
6 F. Barthelat, "Biomimetics for next generation materials", *Philos. Trans. R. Soc. London, Ser. A*, 2007, **365**, 2907–2919.
7 D. K. Dubey and V. Tomar, "Role of molecular level interfacial forces in hard biomaterial mechanics: a review", *Ann. Biomed. Eng.*, 2010, **38**, 2040–2055.
8 M. Yourdkhani, D. Pasini and F. Barthelat, "Multiscale mechanics and optimization of gastropod shells", *J. Bionic Eng.*, 2011, **8**, 357–368.
9 J. H. E. Cartwright and A. G. Checa, "The dynamics of nacre self-assembly", *J. R. Soc. Interface*, 2007, **4**, 491–504.
10 F. D. Fleischli, M. Dietiker, C. Borgia and R. Spolenak, "The influence of internal length scales on mechanical properties in natural nanocomposites: A comparative study on inner layers of seashells", *Acta Biomater.*, 2008, **4**, 1694–1706.
11 D. Verma, K. Katti and D. Katti, "Photoacoustic FTIR spectroscopic study of undisturbed nacre from red abalone", *Spectrochim. Acta, Part A*, 2006, **64**, 1051–1057.
12 K. S. Katti, D. R. Katti, B. Mohanty, "Biomimetic Lessons Learnt from Nacre", in *Biomimetics Learning from Nature*, ed. Amitava Mukherjee, InTech, India, 2010.
13 A. P. Jackson, J. F. V. Vincent and R. M. Turner, "The mechanical design of nacre", *Proc. R. Soc. London, Ser. B*, 1988, **234**, 415–440.
14 M. Sarikaya, K. E. Gunnison, M. Yasrebi and I. A. Aksay, "Mechanical property-microstructural relationships in abalone shell", *MRS Proc.*, 1989, **174**, 109.
15 M. Yasrebi, G. H. Kim, K. E. Gunnison, D. L. Milius, M. Sarikaya and I. A. Aksay, "Biomimetic processing of ceramics and ceramic-metal composites", *MRS Proc.*, 1990, **180**, 625–636.
16 K. E. Gunnison, M. Sarikaya, J. Liu and I. A. Aksay, "Structure-mechanical property relationships in a biological ceramic-polymer composite", *MRS Proc.*, 1991, **255**, 171–184.
17 J. Y. Sun and J. Tong, "Fracture toughness properties of three different biomaterials measured by nanoindentation", *J. Bionic Eng.*, 2007, **4**, 11–17.
18 Z. Y. Tang, N. A. Kotov, S. Magonov and B. Ozturk, "Nanostructured artificial nacre", *Nat. Mater.*, 2003, **2**, 413–418.
19 B. D. Ratner and S. J. Bryant, "Biomaterials: where we have been and where we are going", *Annu. Rev. Biomed. Eng.*, 2004, **6**, 41–75.
20 P. Podsiadlo, S. Paternel, J. M. Rouillard, Z. F. Zhang, J. Lee, J. W. Lee, L. Gulari and N. A. Kotov, "Layer-by-layer assembly of nacre-like nanostructured composites with antimicrobial properties", *Langmuir*, 2005, **21**, 11915–11921.
21 P. Podsiadlo, A. K. Kaushik, E. M. Arruda, A. M. Waas, B. S. Shim, J. D. Xu, H. Nandivada, B. G. Pumplin, J. Lahann, A. Ramamoorthy and N. A. Kotov, "Ultrastrong and stiff layered polymer nanocomposites", *Science*, 2007, **318**, 80–83.
22 F. Barthelat, "Nacre from mollusk shells: a model for high-performance structural materials", *Bioinspir. Biomim.*, 2010, **5**, 035001–1-8.
23 L. J. Bonderer, A. R. Studart and L. J. Gauckler, "Bioinspired design and assembly of platelet reinforced polymer films", *Science*, 2008, **319**, 1069–1073.
24 R. F. Chen, C. A. Wang, Y. Huang and H. R. Le, "An efficient biomimetic process for fabrication of artificial nacre with ordered-nano structure", *Mater. Sci. Eng., C*, 2008, **28**, 218–222.
25 M. A. Meyers, A. Y. M. Lin, P. Y. Chen and J. Muyco, "Mechanical strength of abalone nacre: role of the soft organic layer", *J. Mech. Behav. Biomed. Mater.*, 2008, **1**, 76–85.

26 M. A. Meyers, P. Y. Chen, M. I. Lopez, Y. Seki and A.Y.M. Lin, "Biological materials: A materials science approach", *J. Mech. Behav. Biomed. Mater.*, 2011, **4**, 626–657.
27 B. Bhushan, "Biomimetics: lessons from nature—an overview", *Philos. Trans. R. Soc. London, Ser. A*, 2009, **367**, 1445–1486.
28 G. M. Luz and J. F. Mano, "Biomimetic design of materials and biomaterials inspired by the structure of nacre", *Philos. Trans. R. Soc. London, Ser. A*, 2009, **367**, 1587–1605.
29 G. M. Luz and J. F. Mano, "Mineralized structures in nature: Examples and inspirations for the design of new composite materials and biomaterials", *Compos. Sci. Technol.*, 2010, **70**, 1777–1788.
30 K. S. Liu and L. Jiang, "Bio-inspired design of multiscale structures for function integration", *Nano Today*, 2011, **6**, 155–175.
31 F. Barthelat, C.M. Li, C. Comi and H. D. Espinosa, "Mechanical properties of nacre constituents and their impact on mechanical performance", *J. Mater. Res.*, 2006, **21**, 1977–1986.
32 M. A. Meyers, P. Y. Chen, A.Y.M. Lin and Y. Seki, "Biological materials: Structure and mechanical properties", *Prog. Mater. Sci.*, 2008, **53**, 1–206.
33 T. E. Schäffer, C. IonescuZanetti, R. Proksch, M. Fritz, D. A. Walters, N. Almqvist, C. M. Zaremba, A. M. Belcher, B. L. Smith, G. D. Stucky, D. E. Morse and P. K. Hansma, "Does abalone nacre form by heteroepitaxial nucleation or by growth through mineral bridges?", *Chem. Mater.*, 1997, **9**, 1731–1740.
34 F. Song and Y. L. Bai, "Mineral bridges of nacre and its effects", *Acta Mech. Sin.*, 2001, **17**, 251–257.
35 F. Song, X. H. Zhang and Y. L. Bai, "Microstructure and characteristics in the organic matrix layers of nacre", *J. Mater. Res.*, 2002, **17**, 1567–1570.
36 F. Song, A. K. Soh and Y. L. Bai, "Structural and mechanical properties of the organic matrix layers of nacre", *Biomaterials*, 2003, **24**, 3623–3631.
37 A. G. Checa, J. H. E. Cartwright and M. G. Willinger, "Mineral bridges in nacre", *J. Struct. Biol.*, 2011, **176**, 330–339.
38 X. D. Li, Z. H. Xu and R. Z. Wang, "In situ observation of nanograin rotation and deformation in nacre", *Nano Lett.*, 2006, **6**, 2301–2304.
39 C. Ortiz and M. C. Boyce, "Bioinspired structural materials", *Science*, 2008, **319**, 1053–1054.
40 A. G. Evans, Z. Suo, R. Z. Wang, I. A. Aksay, M. Y. He and J. W. Hutchinson, "Model for the robust mechanical behavior of nacre", *J. Mater. Res.*, 2001, **16**, 2475–2484.
41 K. S. Katti, D. R. Katti, S. M. Pradhan and A. Bhosle, "Platelet interlocks are the key to toughness and strength in nacre", *J. Mater. Res.*, 2005, **20**, 1097–1100.
42 R. Z. Wang and H. S. Gupta, "Deformation and fracture mechanisms of bone and nacre", *Annu. Rev. Mater. Res.*, 2011, **41**, 41–73.
43 F. Heinemann, M. Launspach, K. Gries and M. Fritz, "Gastropod nacre: structure, properties and growth—biological, chemical and physical basics", *Biophys. Chem.*, 2011, **153**, 126–153.
44 S. Bechtle, S.F. Ang and G. A. Schneider, "On the mechanical properties of hierarchically structured biological materials", *Biomaterials*, 2010, **31**, 6378–6385.
45 J. D. Currey, "Mechanical properties of mother of pearl in tension", *Proc. R. Soc. London, Ser. B*, 1977, **196**, 443–463.
46 R. Menig, M. H. Meyers, M. A. Meyers and K. S. Vecchio, "Quasi-static and dynamic mechanical response of *Haliotis rufescens* (abalone) shells", *Acta Mater.*, 2000, **48**, 2383–2398.
47 F. Barthelat and H. D. Espinosa, "An experimental investigation of deformation and fracture of nacre–mother of pearl", *Exp. Mech.*, 2007, **47**, 311–324.
48 F. Barthelat, H. Tang, P. D. Zavattieri, C. M. Li and H. D. Espinosa, "On the mechanics of mother-of-pearl: A key feature in the material hierarchical structure", *J. Mech. Phys. Solids*, 2007, **55**, 306–337.
49 B. J. F. Bruet, H. J. Qi, M. C. Boyce, R. Panas, K. Tai, L. Frick and C. Ortiz, "Nanoscale morphology and indentation of individual nacre tablets from the gastropod mollusc *Trochus niloticus*", *J. Mater. Res.*, 2005, **20**, 2400–2419.
50 K. S. Katti, B. Mohanty and D. R. Katti, "Nanomechanical properties of nacre", *J. Mater. Res.*, 2006, **21**, 1237–1242.
51 B. Mohanty, K. S. Katti, D. R. Katti and D. Verma, "Dynamic nanomechanical response of nacre", *J. Mater. Res.*, 2006, **21**, 2045–2051.
52 B. Bhushan, *Springer Handbook of Nanotechnology*, Springer-Verlag, Heidelberg, Germany, 3rd edn, 2010.
53 B. Bhushan, *Biomimetics: Bioinspired Hierarchical-Structured Surfaces for Green Science and Technology*, Springer-Verlag, Heidelberg, Germany, 2012.
54 X. D. Li, W. C. Chang, Y. J. Chao, R. Wang and M. Chang, "Nanoscale structural and mechanical characterization of a natural nanocomposite material: the shell of red abalone", *Nano Lett.*, 2004, **4**, 613–617.
55 A. Sellinger, P. M. Weiss, A. Nguyen, Y. F. Lu, R. A. Assink, W. L. Gong and C. J. Brinker, "Continuous self-assembly of organic–inorganic nanocomposite coatings that mimic nacre ", *Nature*, 1998, **394**, 256–260.
56 M. Rubner, "Synthetic sea shell", *Nature*, 2003, **423**, 925–926.
57 S. M. Zhang, J. W. Zhang, Z. J. Zhang, H. X. Dang, W. M. Liu and Q. J. Xue, "Preparation and characterization of self-assembled organic-inorganic nacre-like nanocomposite thin films", *Mater. Lett.*, 2004, **58**, 2266–2269.
58 X. Zhang, C. L. Liu, W. J. Wu and J. F. Wang, "Evaporation-induced self-assemblyof organic–inorganic ordered nanocomposite thin films that mimic nacre", *Mater. Lett.*, 2006, **60**, 2086–2089.
59 S. Deville, E. Saiz, R. K. Nalla and A. P. Tomsia, "Freezing as a path to build complex composites", *Science*, 2006, **27**, 515–518.
60 P. Podsiadlo, A. K. Kaushik, B. S. Shim, A. Agarwal, Z. Tang, A. M. Waas, E. M. Arruda and N. A. Kotov, "Can nature's design be improved upon? High strength, transparent nacre-like nanocomposites with double network of sacrificial cross links", *J. Phys. Chem. B*, 2008, **112**, 14359–14363.
61 A. Walther, I. Bjurhager, J.-M. Malho, J. Ruokolainen, L. Berglund and O. Ikkala, "Supramolecular control of stiffness and strength in lightweight high-performance nacre-mimetic paper with fire-shielding properties", *Angew. Chem., Int. Ed.*, 2010, **49**, 6448–6453.
62 N. P. Padture, D. C. Pender, S. Wuttiphan and B. R. Lawn, "In situ processing of silicon carbide layer structures", *J. Am. Ceram. Soc.*, 1995, **78**, 3160–3162.
63 L. Zhang and V. D. Krstic, "High toughness silicon carbide/graphite laminar composite by slip casting", *Theor. Appl. Fract. Mech.*, 1995, **24**, 13–19.
64 C. A. Wang, Y. Huang, Q. F. Zan, H. Guo and S.Y. Cai, "Biomimetic structure design—a possible approach to change the brittleness of ceramics in nature", *Mater. Sci. Eng., C*, 2000, **11**, 9–12.
65 G. Mayer, "Rigid biological systems as models for synthetic composites", *Science*, 2005, **310**, 1144–1147.
66 G. Mayer, "New classes of tough composite materials—lessons from natural rigid biological systems", *Mater. Sci. Eng., C*, 2006, **26**, 1261–1268.
67 H. Wei, N. Ma, F. Shi, Z. Q. Wang and X. Zhang, "Artificial nacre by alternating preparation of layer-by-layer polymer films and $CaCO_3$ strata", *Chem. Mater.*, 2007, **19**, 1974–1978.
68 A. Y. M. Lin, P. Y. Chen and M. A. Meyers, "The growth of nacre in the abalone shell", *Acta Biomater.*, 2008, **4**, 131–138.
69 E. Munch, M. E. Launey, D. H. Alsem, E. Saiz, A. P. Tomsia and R. O. Ritchie, "Tough bio-inspired hybrid materials", *Science*, 2008, **322**, 1516–1520.
70 S. Bueno and C. Baudín, "Design and processing of a ceramic laminate with high toughness and strong interfaces", *Composites, Part A*, 2009, **40**, 137–143.
71 T. H. Lin, W. H. Huang, I. K. Jun and P. Jiang, "Bioinspired assembly of colloidal nanoplatelets by electric field", *Chem. Mater.*, 2009, **21**, 2039–2044.
72 M. E. Launey, E. Munch, D. H. Alsem, E. Saiz, A. P. Tomsia and R. O. Ritchie, "A novel biomimetic approach to the design of high-performance ceramic–metal composites", *J. R. Soc. Interface*, 2010, **7**, 741–753.
73 H. Kakisawa and T. Sumitomo, "The toughening mechanism of nacre and structural materials inspired by nacre", *Sci. Technol. Adv. Mater.*, 2011, **12**, 064710–1-14.
74 D. R. Katti and K. S. Katti, "3D finite element modeling of mechanical response in nacre-based hybrid nanocomposites", *J. Mater. Sci.*, 2001, **36**, 1411–1417.
75 K. Okumura and P. G. de Gennes, "Why is nacre strong? Elastic theory and fracture mechanics for biocomposites with stratified structures", *Eur. Phys. J. E: Soft Matter Biol. Phys.*, 2001, **4**, 121–127.
76 K. S. Katti, D.R. Katti, J. Tang, S. Pradhan and M. Sarikaya, "Modeling mechanical responses in a laminated biocomposite. Part

II. Nonlinear responses and nuances of nanostructure", *J. Mater. Sci.*, 2005, **40**, 1749–1755.
77 H. J. Gao, "Application of fracture mechanics concepts to hierarchical biomechanics of bone and bone-like materials", *Int. J. Fract.*, 2006, **138**, 101–137.
78 H. Tang, F. Barthelat and H.D. Espinosa, "An elasto-viscoplastic interface model for investigating the constitutive behavior of nacre", *J. Mech. Phys. Solids*, 2007, **55**, 1410–1438.
79 A. Y. M. Lin, *Structural and functional biological materials: abalone nacre, sharp materials, and abalone foot adhesion*. PhD thesis, University of California, San Diego, 2008.
80 K. Tushtev, M. Michael and G. Georg, "On the nature of the stiffness of nacre", *Mater. Sci. Eng., C*, 2008, **28**, 1164–1172.
81 C. Hedegaard, "Shell structures of the recent Vetigastropoda", *J. Molluscan Stud.*, 1997, **63**, 369–377.
82 C. Hedegaard and H. Wenk, "Microstructure and texture patterns of mollusc shells", *J. Molluscan Stud.*, 1998, **64**, 133–136.
83 D. Chateigner, C. Hedegaard and H. Wenk, "Mollusc shell microstructures and crystallographic textures", *J. Struct. Geol.*, 2000, **22**, 1723–1735.
84 S. Blank, M. Arnoldi, S. Khoshnavaz, L. Treccani, M. Kuntz, K. Mann, G. Grathwohl and M. Fritz, "The nacre protein perlucin nucleates growth of calcium carbonate crystals", *J. Microsc.*, 2003, **212**, 280–291.
85 L. Qiao, Q.L. Feng and S.S. Lu, "In vitro growth of nacre-like tablet forming: From amorphous calcium carbonate, nanostacks to hexagonal tablets", *Cryst. Growth Des.*, 2008, **8**, 1509–1514.
86 M. A. Meyers, C. T. Lim, A. B. R. Li, H. Nizam, E. P. S. Tan, Y. Seki and J. McKittrick, "The role of organic intertile layer in abalone nacre", *Mater. Sci. Eng. C*, 2009, **29**, 2398–2410.
87 M. Fritz, A. M. Belcher, M. Radmacher, D. A. Walters, P. K. Hansma, G. D. Strucky and D. E. Morse, "Flat pearls from biofabrication of organized composites on inorganic substrates", *Nature*, 1994, **371**, 49–51.
88 F. Nudelman, B. A. Gotliv, L. Addadi and S. Weiner, "Mollusk shell formation: Mapping the distribution of organic matrix components underlying a single aragonitic tablet in nacre", *J. Struct. Biol.*, 2006, **153**, 176–187.
89 H. Nakahara, "Nacre formation in bivalve and gastropod molluscs", in *Mechanisms and Phylogeny of Mineralization in Biological Systems*, ed. S. Suga and H. Nakahara, Springer-Verlag, Tokyo, 1991, pp. 343–350.
90 S. Weiner and L. Addadi, "Design strategies in mineralized biological materials", *J. Mater. Chem.*, 1997, **7**, 689–702.
91 A. Y. M. Lin and M. A. Meyers, "Growth and structure in abalone shell", *Mater. Sci. Eng., A*, 2005, **390**, 27–41.
92 D. J. Jackson, C. McDougall, B. Woodcroft, P. Moase, R. A. Rose, M. Kube, R. Reinhardt, D. S. Rokhsar, C. Montagnani, C. Joubert, D. Piquemal and B. M. Degnan, "Parallel evolution of nacre building gene sets in molluscs", *Mol. Biol. Evol.*, 2010, **27**, 591–608.
93 L. P. Xie, F. J. Zhu, Y. J. Zhou, C. Yang and R. Q. Zhang, "Molecular approaches to understand biomineralization of shell nacreous layer", *Prog Mol Subcell Biol*, 2011, **52**, 331–352.
94 A. G. Checa, J. H. E. Cartwright and M. G. Willinger, "The key role of the surface membrane in why gastropod nacre grows in towers", *Proc. Natl. Acad. Sci. U. S. A.*, 2009, **106**, 38–43.
95 D. Verma, K. Katti and D. Katti, "Nature of water in nacre: a 2D Fourier transform infrared spectroscopic study", *Spectrochim. Acta, Part A*, 2007, **67**, 784–788.
96 R. Z. Wang, H. B. Wen, F. Z. Cui, H. B. Zhang and H. D. Li, "Observations of damage morphologies in nacre during deformation and fracture", *J. Mater. Sci.*, 1995, **30**, 2299–2304.
97 M. A. Meyers and K.K. Chawla, *Mechanical behavior of materials*, Cambridge University Press, New York, 2008.
98 B. L. Smith, T. E. Schäffer, M. Viani, J. B. Thompson, N. A. Frederick, J. Kindt, A. Belcher, G. D. Stucky, D. E. Morse and P. K. Hansma, "Molecular mechanistic origin of the toughness of natural adhesive, fibres and composites", *Nature*, 1999, **399**, 761–763.
99 M. Sarikaya, "An introduction to biomimetics: a structural viewpoint", *Microsc. Res. Tech.*, 1994, **27**, 360–375.
100 G. Mayer, "New toughening concepts for ceramic composites from rigid natural materials", *J. Mech. Behav. Biomed. Mater.*, 2011, **4**, 670–681.
101 M. Rousseau, E. Lopez, A. Couté, G. Mascarel, D. C. Smithc, R. Naslaind and X. Bourrat, "Sheet nacre growth mechanism: a Voronoi model", *J. Struct. Biol.*, 2005, **149**, 149–215.
102 N. Yao, A. Epstein and A. Akey, "Crystal growth via spiral motion in abalone shell nacre", *J. Mater. Res.*, 2006, **21**, 1939–1946.
103 J. F. Wang, Q. F. Cheng and Z. Y. Tang, "Layered nanocomposites inspired by the structure and mechanical properties of nacre", *Chem. Soc. Rev.*, 2012, **41**, 1111–1129.
104 F. Barthelat, J. Rim, H. D. Espinosa, "A review on the structure and mechanical properties of mollusk shells—perspectives on synthetic biomimetic materials" in *Applied Scanning Probe Methods XIII*, ed. B. Bhushan and H. Fuchs, Springer, 2009, pp. 1059–1100.
105 J. B. Wachtman, *Mechanical Properties of Ceramics*, Wiley-Interscience, New York, 1996.
106 H. M. Leung and S. K. Sinha, "Scratch and indentation tests on seashells", *Tribol. Int.*, 2009, **42**, 40–49.
107 P. Stempflé and M. Brendlé, "Tribological behaviour of nacre-Influence of the environment on the elementary wear processes", *Tribol. Int.*, 2006, **39**, 1485–1496.
108 P. Stempflé, T. Djilali, R. K. Njiwa, M. Rousseau, E. Lopez and X. Bourrat, "Thermal-induced wear mechanisms of sheet nacre in dry friction", *Tribol. Lett.*, 2009, **35**, 97–104.
109 J. Bezares, Z. L. Peng, R. J. Asaro and Q. Zhu, "Macromolecular structure and viscoelastic response of the organic framework of nacre in *Haliotis rufescens*: a perspective and overview", *Theort. Appl. Mech.*, 2011, **38**, 75–106.
110 H. Moshe-Drezner, D. Shilo, A. Dorogoy and E. Zolotoyabko, "Nanometer-scale mapping of elastic modules in biogenic composites: The nacre of mollusk shells", *Adv. Funct. Mater.*, 2010, **20**, 2723–2728.
111 B. Mohanty, K. S. Katti and D. R. Katti, "Experimental investigation of nanomechanics of the mineral-protein interface in nacre", *Mech. Res. Commun.*, 2008, **35**, 17–23.
112 S. Deville, E. Saiz, A. P. Tomsia, "Using ice to mimic nacre: from structural applications to artificial bone", in *Handbook of Biomineralization: Biomimetic and Bioinspired Chemistry*, ed. P. Behrens and E. Bäuerlein, John Wiley & Sons, Ltd, Weinheim, Germany, 2008.
113 M. Sarikaya, I. A. Aksay, "Nacre of abalone shell: a natural multifunctional nanolaminated ceramic-polymer composite malarial", in *Results and Problems in Cell Differentiation – Biopolymers*, ed. S. T. Case, Springer-Verlag, Berlin, 1992.
114 J. Machado, M. Lopes-Lima, A. Damasceno-Oliveira, A. Colaço, J. Andrade, D. Silva, C. Jiménez-López, A. Rodríguez-Navarro and A. Checa, "The influenceof hydrostatic pressure on shell mineralization of Anodonta cygnea: A comparative study with a hydrothermal vent bivalve Bathymodiolus azoricus", *J. Shellfish Res.*, 2009, **28**, 899–904.
115 B. Pokroy, V. Demensky and E. Zolotoyabko, "Nacre in mollusk shells as a multilayered structure with strain gradient", *Adv. Funct. Mater.*, 2009, **19**, 1054–1059.
116 P. Stempflé, O. Pantalé, M. Rousseau, E. Lopez and X. Bourrat, "Mechanical properties of the elemental nanocomponents of nacre structure", *Mater. Sci. Eng., C*, 2010, **30**, 715–721.
117 J. D. Currey, P. Zioupos, P. Davies and A. Casinos, "Mechanical properties of nacre and highly mineralized bone", *Proc. R. Soc. London, Ser. B*, 2001, **268**, 107–111.
118 F. Z. Ren, X. D. Wan, Z. H. Ma and J. H. Su, "Study on microstructure and thermodynamics of nacre in mussel shell", *Mater. Chem. Phys.*, 2009, **114**, 367–370.
119 F. Song, J. B. Zhou, X. H. Xu, Y. Xu and Y. L. Bai, "Effect of a negative poisson ratio in the tension of ceramics", *Phys. Rev. Lett.*, 2008, **100**, 245502–1-4.
120 J. Bezares, R. J. Asaro and M. Hawley, "Macromolecular structure of the organic framework of nacre in *Haliotis rufescens*: Implications for growth and mechanical behavior", *J. Struct. Biol.*, 2008, **163**, 61–75.
121 A. Y. M. Lin and M. A. Meyers, "Interfacial shear strength in abalone nacre", *J. Mech. Behav. Biomed. Mater.*, 2009, **2**, 607–612.
122 R. Menig, M. H. Meyers, M.A. Meyers and K. S. Vecchio, "Quasi-static and dynamic mechanical response of *Strombus gigas* (conch) shells", *Mater. Sci. Eng.*, 2001, **A297**, 203–211.
123 J. E. Villarreal, *Mapping of elastic modulus and hardness in Trochus niloticus seashell nacre*, Masters thesis, Massachusetts Institute of Technology, Cambridge, Massachusetts, 2007.

